



*Supplement of*

## **Assessing potential indicators of aerosol wet scavenging during long-range transport**

**Miguel Ricardo A. Hilario et al.**

*Correspondence to:* Armin Sorooshian ([armin@arizona.edu](mailto:armin@arizona.edu))

The copyright of individual parts of the supplement might differ from the article licence.

**Table S1: The name of the equation used for each predictor and the resulting coefficients. Only the top eight predictors per panel in Fig. 2 are shown for brevity. Coefficients are formatted as 25<sup>th</sup> / 50<sup>th</sup> / 75<sup>th</sup> percentiles. Mathematical forms of each equation are provided in Table 2. Values are rounded off to three significant figures. Rows are ordered alphabetically by predictor.**

Predictor	Equation	a	b	c	d
APT <sub>72H,IMERG</sub>	Kanaya	72.1 / 218 / 636	-13.9 / -11.8 / -9.83	-0.00396 / -0.00381 / -0.00362	0.0272 / 0.0273 / 0.0278
APT <sub>48H,IMERG</sub>	Kanaya	96.8 / 122 / 135	-48.9 / -46.4 / -42.6	-0.00343 / -0.00315 / -0.00278	0.0268 / 0.0269 / 0.0269
APT <sub>48H,P-CDR</sub>	Kanaya	192 / 708 / 337000	-25.7 / -13.8 / -11.4	-0.00838 / -0.00797 / -0.00773	0.0315 / 0.0319 / 0.0321
APT <sub>72H,P-CDR</sub>	General Exponential	0.00793 / 0.00809 / 0.01	0.0267 / 0.0326 / 0.0421	0.0183 / 0.0199 / 0.0205	-
APT <sub>PCP &gt; 0.2 mm,72H,IMERG</sub>	General Exponential	0.0079 / 0.00934 / 0.0102	1.04 / 1.06 / 1.11	0.0237 / 0.024 / 0.0244	-
APT <sub>12H,GFS</sub>	Kanaya	0.983 / 1.00 / 17.4	-4.28 / -4.01e-05 / -6.32e-06	-0.00522 / -0.00456 / -0.00267	0.0255 / 0.0262 / 0.0263
APT <sub>PCP &gt; 0.2 mm,48H,IMERG,&lt;1500m</sub>	Kanaya	6.27e-07 / 6.67e-07 / 1.27e-06	1.55 / 1.63 / 1.71	-96.5 / -87.4 / -73.1	73.2 / 87.5 / 96.5
APT <sub>24H,GFS</sub>	Kanaya	8.37 / 13.8 / 15.7	24.7 / 107 / 111	0.003 / 0.00341 / 0.00451	0.0235 / 0.0236 / 0.024
RH <sub>q90</sub>	Gaussian	0.0335 / 0.0345 / 0.0353	83.9 / 83.9 / 83.9	5.56 / 5.59 / 5.69	0.0101 / 0.0102 / 0.0103
RH <sub>q95</sub>	Gaussian	0.0354 / 0.0356 / 0.0359	85.3 / 85.3 / 85.4	5.84 / 5.9 / 5.94	0.00911 / 0.00953 / 0.0096
RH <sub>q50</sub>	Gaussian	0.0299 / 0.0306 / 0.0309	77.8 / 77.9 / 77.9	4.13 / 4.33 / 4.36	0.0141 / 0.0141 / 0.0145
RH <sub>q100</sub>	Gaussian	0.0349 / 0.0353 / 0.0361	87.6 / 87.8 / 88	6.32 / 6.39 / 6.49	0.00786 / 0.00829 / 0.00853
RH <sub>q85</sub>	Gaussian	0.0307 / 0.0316 / 0.0321	82.7 / 82.7 / 82.8	5.21 / 5.37 / 5.47	0.0114 / 0.0116 / 0.0118
RH <sub>mean</sub>	Gaussian	0.0306 / 0.0314 / 0.0316	76.9 / 77 / 77	4.9 / 4.98 / 5.11	0.013 / 0.0132 / 0.0133
f <sub>MR15</sub>	Kanaya	1.62 / 1.83 / 2.66	0.445 / 0.468 / 0.595	-0.0505 / -0.0482 / -0.0427	0.0567 / 0.0621 / 0.0646
f <sub>RH95</sub>	Kanaya	-0.00413 / -0.00306 / 15.2	0.537 / 0.553 / 1.06	-15 / -11.4 / -2.53	2.56 / 11.4 / 15.1
PA <sub>72H,P-CDR</sub>	Kanaya	-1.73 / -0.0213 / -0.0113	0.136 / 0.378 / 0.591	-0.865 / -0.39 / -0.0242	0.0598 / 0.419 / 0.893
PA <sub>48H,P-CDR</sub>	General Exponential	0.0162 / 0.0179 / 0.0211	0.826 / 0.973 / 1.07	0.00794 / 0.0109 / 0.0121	-
PA <sub>24H,GFS</sub>	General Exponential	-0.0159 / 0.408 / 2.45	-0.0577 / 0.00174 / 0.00888	-2.42 / -0.381 / 0.0423	-
PA <sub>12H,P-CDR</sub>	Kanaya	0.679 / 0.719 / 0.806	-1.03e-05 / 4.43e-07 / 1.08e-06	-0.00169 / 0.00985 / 0.011	0.0186 / 0.0197 / 0.0252
PA <sub>12H,GFS</sub>	General Exponential	7.91 / 9.17 / 10.6	0.000326 / 0.000394 / 0.000491	-10.6 / -9.14 / -7.89	-
PA <sub>PCP &gt; 0.2 mm,48H,P-CDR,&lt;1500m</sub>	Kanaya	355 / 541 / 1260	9.22 / 9.73 / 11.1	0.0148 / 0.0157 / 0.0167	0.0361 / 0.0363 / 0.0364
PA <sub>24H,P-CDR</sub>	General Exponential	14.8 / 16.8 / 18.7	0.00054 / 0.000631 / 0.000704	-18.7 / -16.8 / -14.7	-
PA <sub>12H,IMERG,&lt;1500m</sub>	General Exponential	18.9 / 20.3 / 26.8	0.000285 / 0.000345 / 0.000434	-26.8 / -20.2 / -18.9	-
PF <sub>PCP &gt; 0.2 mm,72H,P-CDR,&lt;1500m</sub>	Kanaya	0.00196 / 0.00279 / 0.00385	3.2 / 3.48 / 3.69	-76.5 / -48.3 / -35.6	35.6 / 48.4 / 76.6
PF <sub>PCP &gt; 0.2 mm,48H,P-CDR,&lt;1500m</sub>	Kanaya	0.000784 / 0.000827 / 0.00092	4.38 / 4.61 / 4.66	-156 / -147 / -135	135 / 147 / 156
PF <sub>48H,IMERG</sub>	General Exponential	-2.31 / -1.51 / -1.44	-0.00307 / -0.0027 / -0.00224	1.47 / 1.53 / 2.33	-
PF <sub>72H,IMERG</sub>	General Exponential	-0.885 / 0.00681 / 0.0124	0.193 / 1.28 / 2.09	0.0155 / 0.021 / 0.912	-
PF <sub>12H,IMERG</sub>	General Exponential	0.661 / 1.08 / 1.49	0.00324 / 0.004 / 0.00933	-1.46 / -1.05 / -0.635	-

PF <sub>24H,IMERG</sub>	General Exponential	0.728 / 1.01 / 1.38	0.00517 / 0.00725 / 0.00852	-1.35 / -0.982 / -0.702	-
PF <sub>72H,GFS</sub>	General Exponential	0.365 / 0.565 / 0.871	0.000513 / 0.00245 / 0.0029	-0.846 / -0.54 / -0.339	-
PI <sub>PCP &gt; 0.2 mm,12H,IMERG,&lt;1500m</sub>	Gaussian	-622 / -587 / -562	0.4 / 0.404 / 0.408	-30.7 / -29.9 / -29.2	562 / 587 / 622
PI <sub>PCP &gt; 0.2 mm,48H,P-CDR</sub>	Kanaya	13.8 / 15.7 / 16.3	2.83 / 3 / 3.22	0.259 / 0.285 / 0.299	0.0197 / 0.02 / 0.0202
PI <sub>PCP &gt; 0.2 mm,48H,P-CDR,&lt;1500m</sub>	Kanaya	2.86 / 2.99 / 3.19	0.83 / 0.88 / 0.941	0.38 / 0.438 / 0.511	0.0299 / 0.0304 / 0.0307
PI <sub>PCP &gt; 0.2 mm,72H,P-CDR,&lt;1500m</sub>	General Exponential	0.306 / 0.322 / 0.332	2.23 / 2.29 / 2.36	0.0314 / 0.0315 / 0.0319	-
PI <sub>PCP &gt; 0.2 mm,72H,P-CDR</sub>	Kanaya	175 / 232 / 542	9.65 / 10.2 / 11.9	0.129 / 0.132 / 0.136	0.0208 / 0.0211 / 0.0213
PI <sub>PCP &gt; 0.2 mm,24H,P-CDR,&lt;1500m</sub>	General Exponential	1.24 / 1.33 / 1.42	6.61 / 6.79 / 7.01	0.035 / 0.0358 / 0.0362	-
PI <sub>PCP &gt; 0.2 mm,24H,P-CDR</sub>	General Exponential	11.1 / 12.0 / 13.9	13.0 / 13.3 / 13.6	0.0194 / 0.0196 / 0.02	-
PI <sub>PCP &gt; 0.2 mm,48H,GFS</sub>	Gaussian	-0.0111 / -0.0109 / -0.0101	1.99 / 2.11 / 2.21	1.43 / 1.46 / 1.54	0.0317 / 0.0319 / 0.0321
PI <sub>72H,P-CDR,&lt;1500m</sub>	General Exponential	0.0358 / 0.0365 / 0.0378	0.43 / 0.454 / 0.478	0.0142 / 0.0146 / 0.0153	-

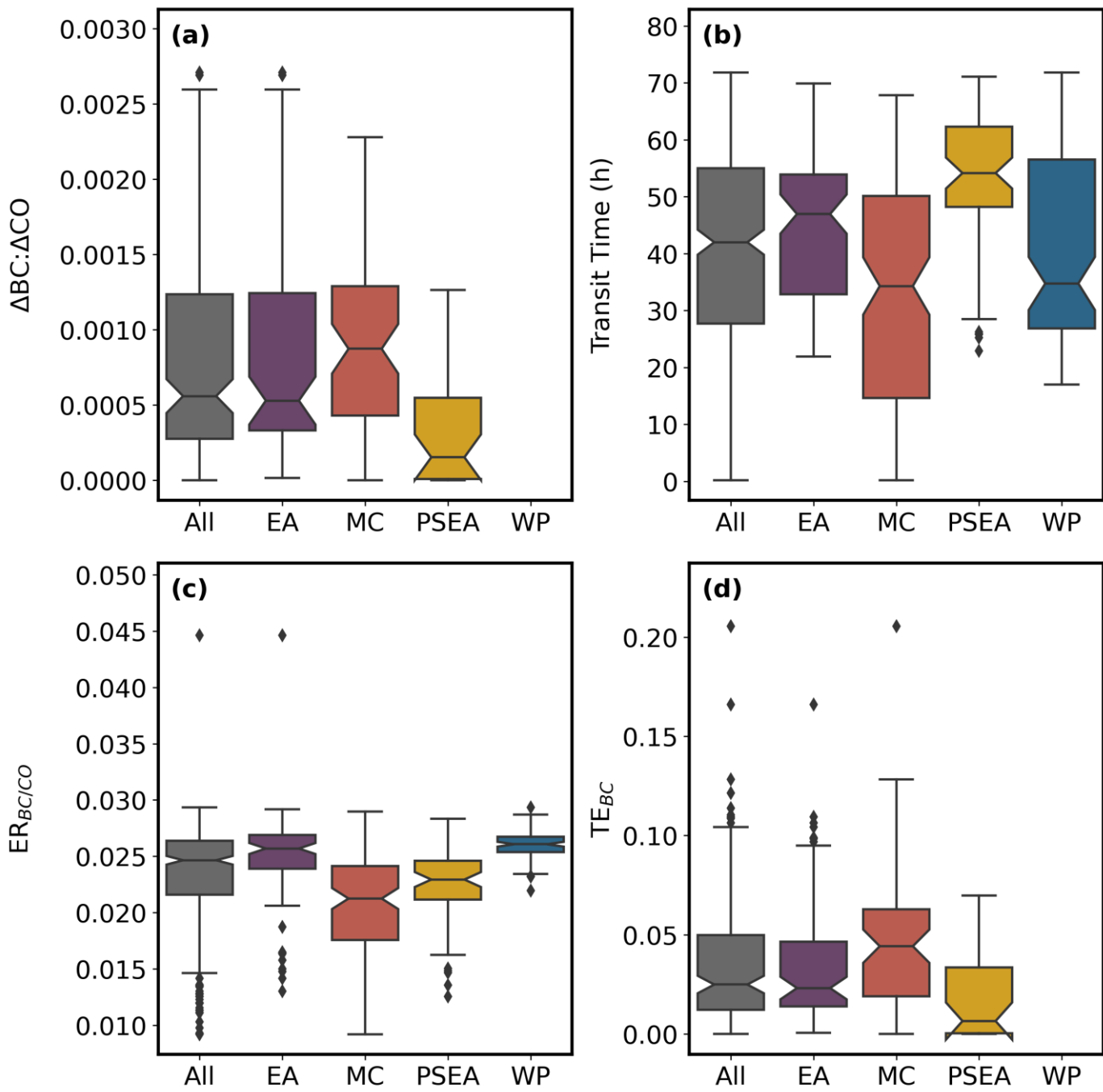
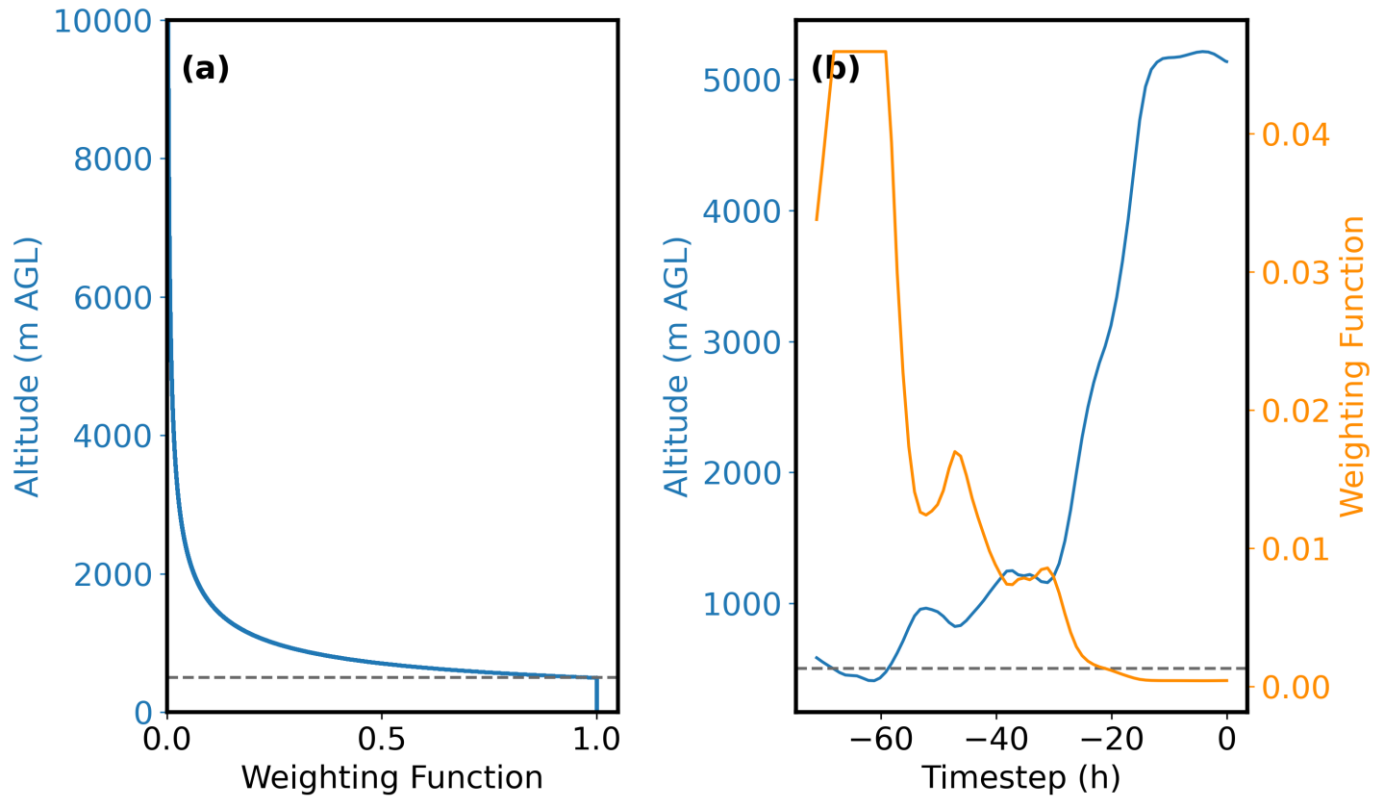


**Figure S1:** (a) The enhancement ratio of black carbon (BC) to carbon monoxide (CO) ( $\Delta BC/\Delta CO$ ; unitless) per source region (EA: East Asia, MC: Maritime Continent, PSEA: Peninsular Southeast Asia, WP: West Pacific; identified in Hilario et al. (2021)), (b) transit times (in hours) from major source regions, (c) emission ratios of BC/CO ( $ER_{BC/CO}$ ) along each trajectory using the CAMS-GLOB-ANT emissions (Sect. 2.4-2.5), and (d) transport efficiencies of BC ( $TE_{BC}$ ). Boxplots for WP in (a) and (d) were removed due to a low number of data points ( $N = 2$ ) remaining after the  $\Delta CO > 0.02$  ppm filter (Sect. 2.2). Note that in (a), CO was converted from ppm to  $\mu\text{g m}^{-3}$  using the ambient pressure and temperature measured by the aircraft such that  $\Delta BC/\Delta CO$  would be unitless.



25

**Figure S2:** (a) Weighting function used when calculating average emission ratios along trajectories, assuming a well-mixed environment below 500 m (dashed gray line). (b) An example trajectory that shows the inverse relationship between trajectory altitude (left Y-axis, blue) and assigned weight (right Y-axis, orange) over trajectory timestep (X-axis). A timestep of 0 refers to when the trajectory reaches the aircraft location. Before calculating the average emission ratio, weights in (b) are normalized such that the area under the weighting function is equal to 1.

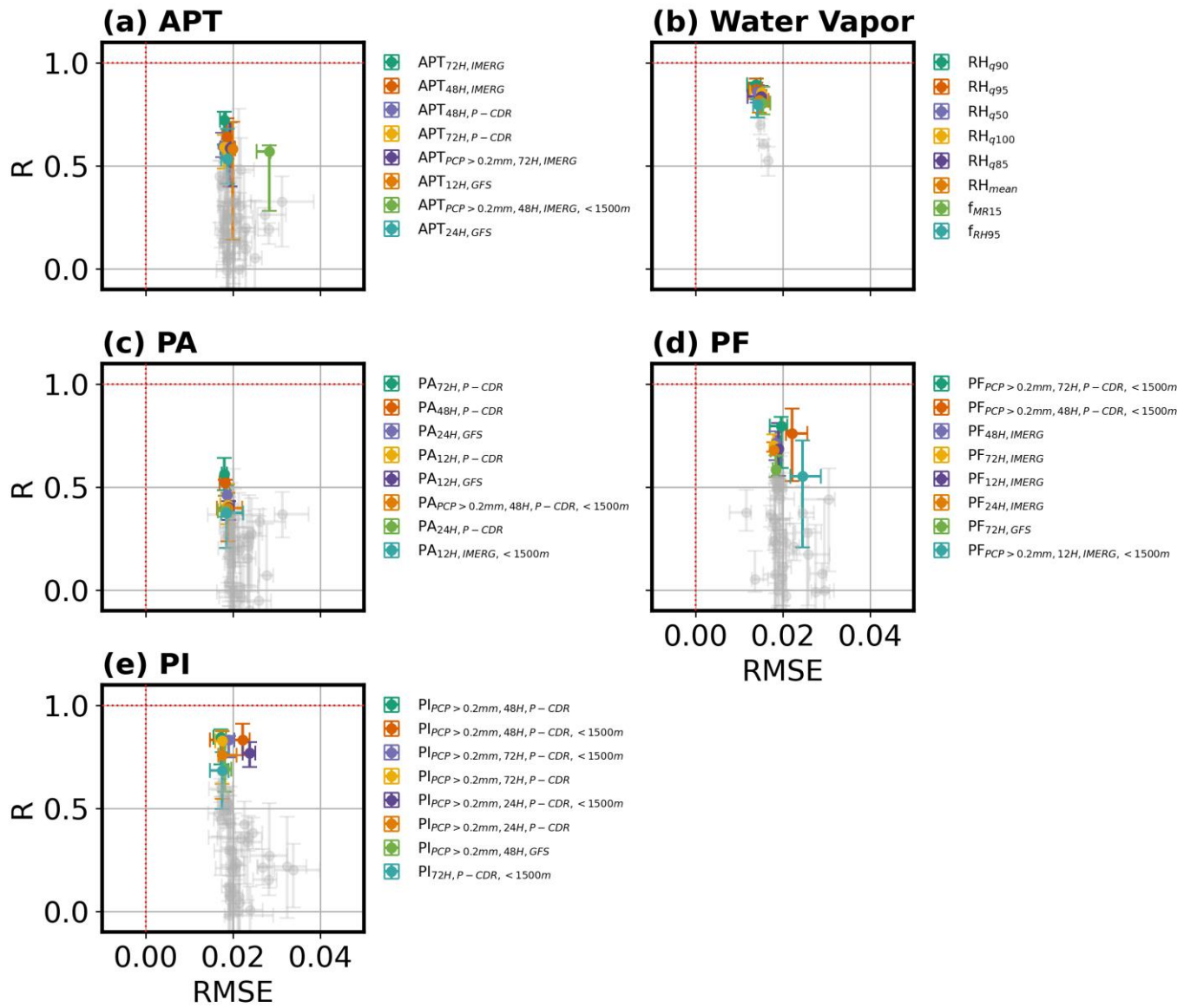
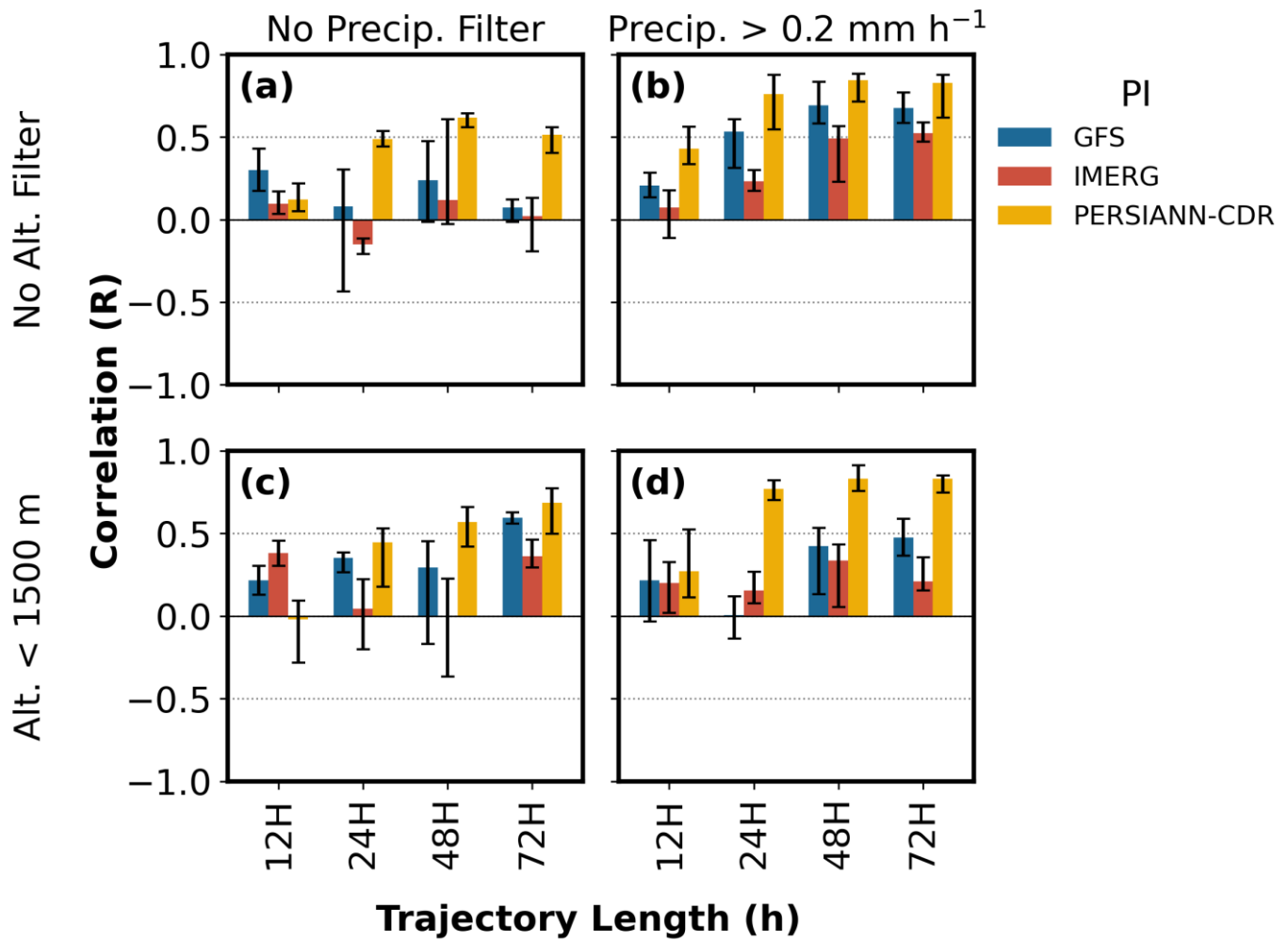


**Figure S3:** Root mean squared error (RMSE) and Pearson R derived from linear regressions of observed (x) and predicted (y)  $\Delta\text{BC}/\Delta\text{CO}$  with error bars representing the 25<sup>th</sup> and 75<sup>th</sup> percentile values derived from k-fold cross validation (k=10). Ideal values are denoted by the red dashed lines such that a better predictor would fall closer to the intersection of the two lines. Only predictors with median R > 0.71 are shown. Note that PERSIANN-CDR has been abbreviated to P-CDR (b-c). Panels share the same X- and Y-axis limits.



40

Figure S4: Pearson correlations ( $R$ ) between observed  $TE_{BC}$  and  $TE_{BC}$  predicted by precipitation intensity (PI) for different trajectory lengths and precipitation data products. Each panel refers to a combination of altitude and precipitation intensity filters. Panels share the same X- and Y-axis limits.

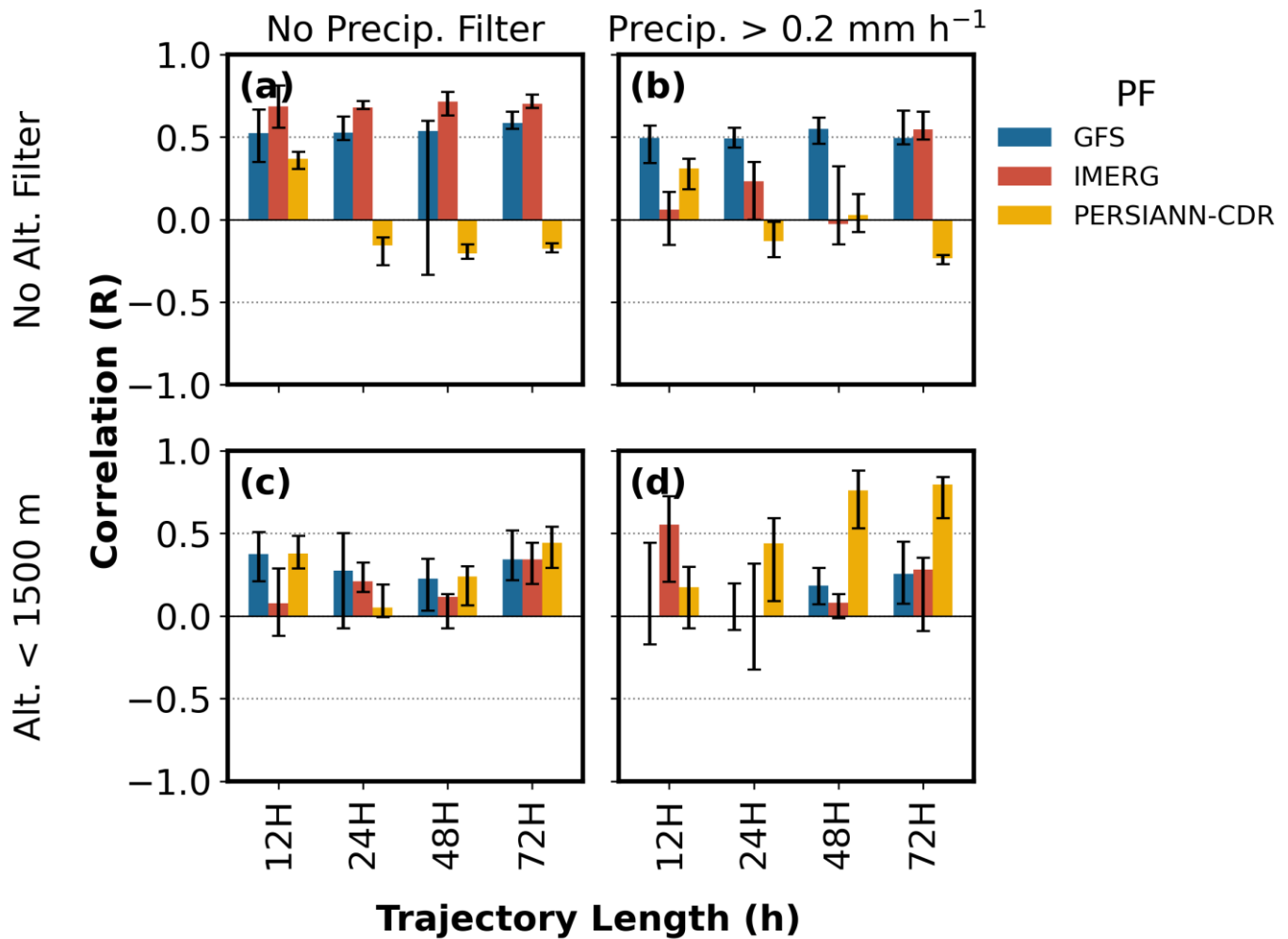


Figure S5: Same as Fig. S4 but for precipitation frequency (PF).

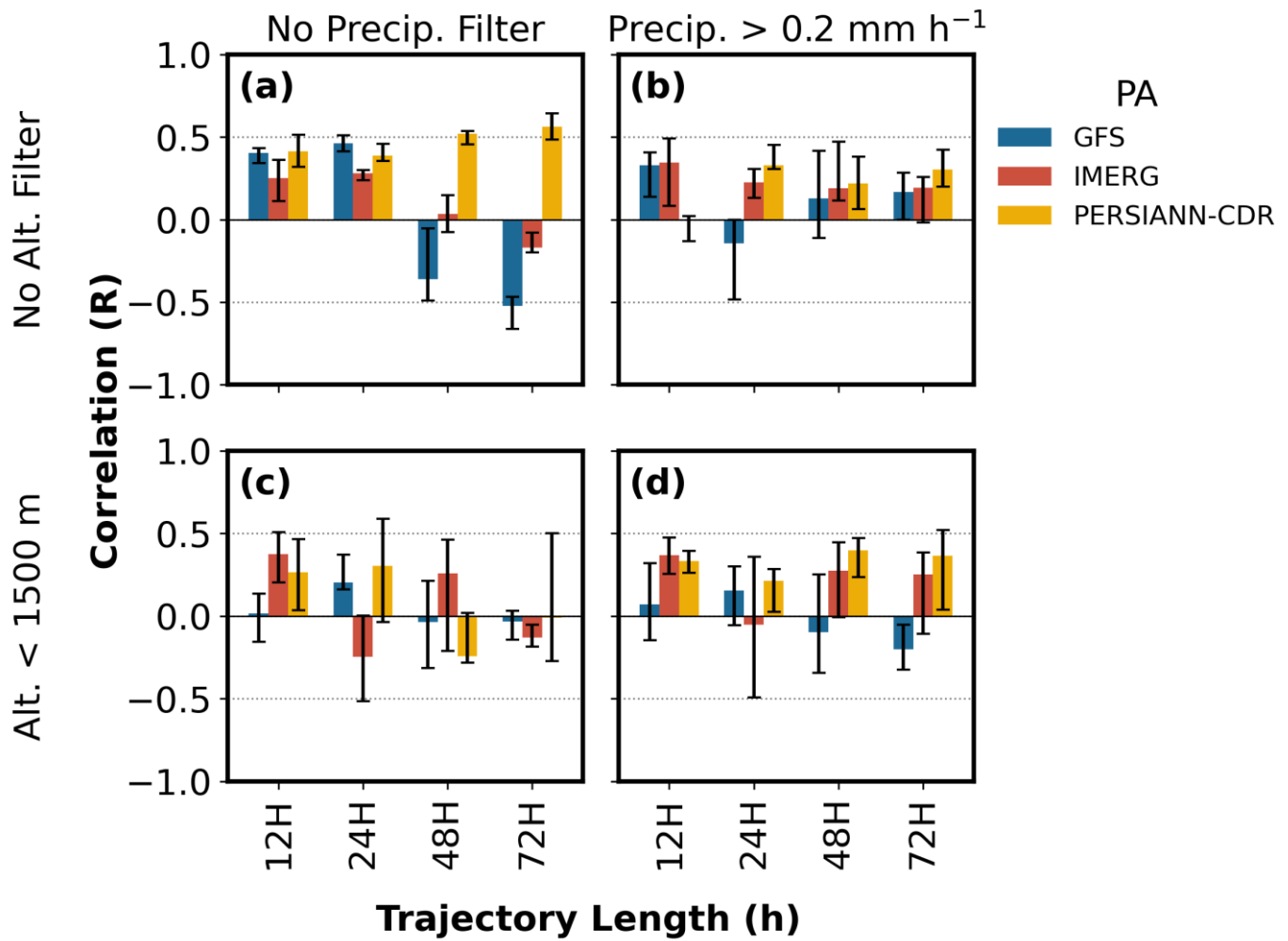


Figure S6: Same as Fig. S4 but for precipitation amount (PA).

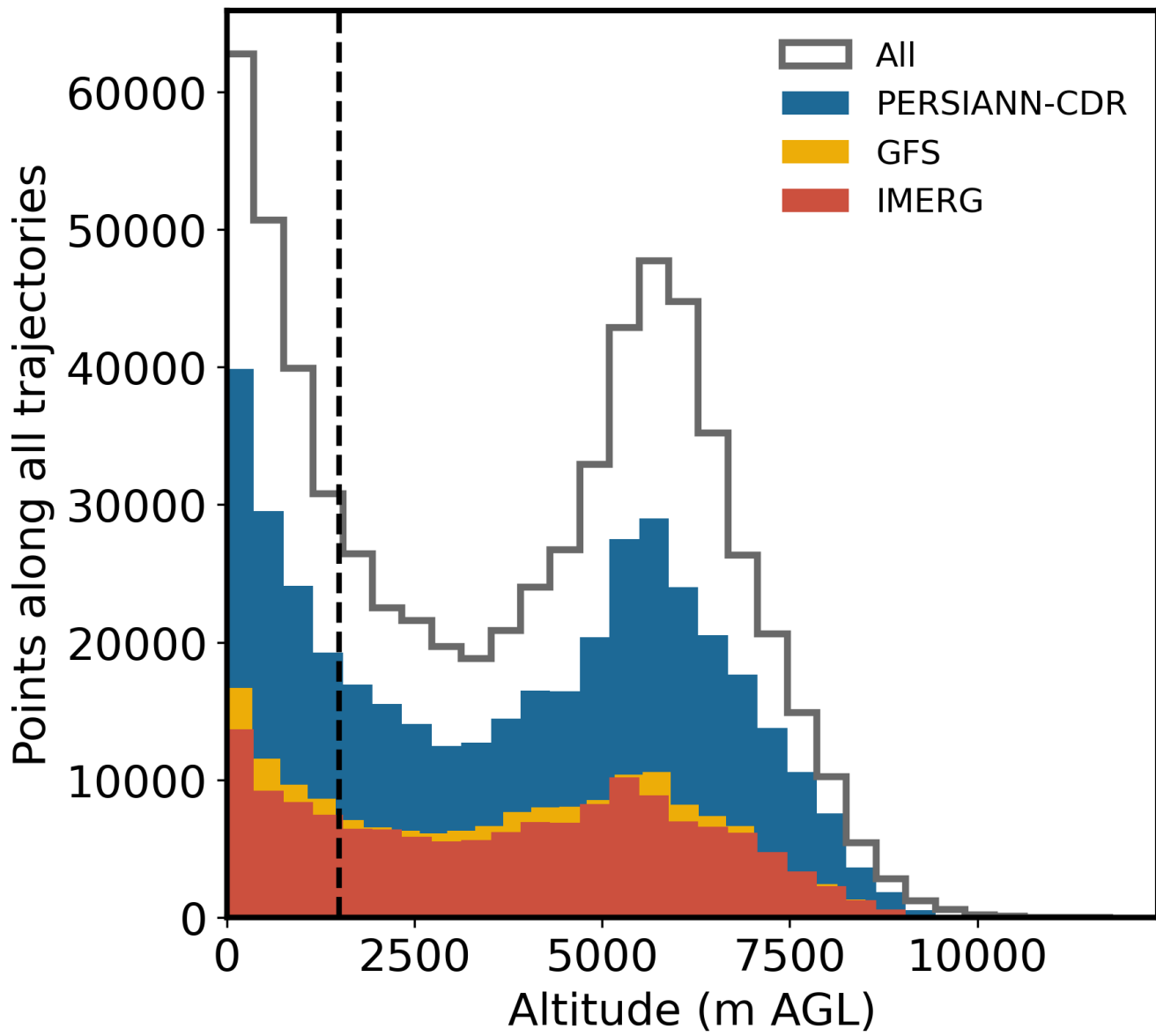


Figure S7: Histograms of trajectory altitude (m AGL) for all points along the 72-h backward trajectories (gray) and for points with non-zero precipitation based on PERSIANN-CDR (blue), GFS (yellow), and IMERG (red) (not stacked). The vertical dashed line shows the 1.5 km filter threshold used when calculating precipitation variables.